ACS Catalysis

Research Article

pubs.acs.org/acscatalysis

Origins of the Regioselectivity in the Lutetium Triflate Catalyzed Ketalization of Acetone with Glycerol: A DFT Study

Aaron W. Pierpont,*[,†] Enrique R. Batista,[†] Richard L. Martin,[†] Weizhong Chen,[‡,∥] Jin Kyung Kim,[§,⊥] Caroline B. Hoyt,[§,#] John C. Gordon,*[,‡] Ryszard Michalczyk,[§] Louis A. "Pete" Silks,[§] and Ruilian Wu[§]

[†]Theoretical Division, [‡]Chemistry Division, and [§]Bioscience Division, Los Alamos National Laboratory, Los Alamos, New Mexico 87545, United States

Supporting Information

ABSTRACT: We describe DFT computations that address the regioselective preference toward the five-membered ring product 1,3-dioxolane (solketal) over the six-membered-ring product (1,3-dioxane) during $Lu(OTf)_3$-catalyzed ketalization of acetone with glycerol. When ketalization occurs via the internal (secondary) −OH group of glycerol, only solketal production should be possible due to the symmetry of the intermediates. Ketalization via the terminal −OH group of glycerol is predicted to occur in a different manner than the conventionally proposed ketalization mechanism. A constrained hemiketal intermediate is invoked to explain the selectivity for solketal formation.

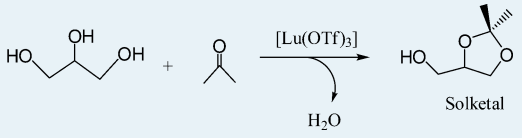

KEYWORDS: *glycerol, solketal, regioselective, Lewis acid, catalysis*

INTRODUCTION

Worldwide production of biodiesel via transesterification of animal fats/vegetable oils has increased steadily to 13 million tons/year over the last few decades due to its lower toxicity and higher biodegradability in comparison to petroleum-based fuels.[1] One of the main drawbacks to industrial-scale biodiesel production, however, is that 10 tons of glycerol byproduct are produced for every 100 tons of biodiesel, which amounts to 2.0 million tons of glycerol per year on a global scale.[2] As a result, glycerol prices have remained relatively low and some biodiesel producers have encountered serious financial difficulties due to the high costs of disposing of excess glycerol.[3] Both of these factors (low glycerol price and high disposal costs) have generated increased interest in using glycerol as a chemical feedstock.

Although glycerol itself has been shown to be a promising precursor to a variety of valuable oxygenates via oxidation, dehydration, hydrogenation, etherification, and esterification,[4] its utility is limited by physical (high viscosity and hydrophilicity) and chemical properties (three hydroxyl groups in close proximity). As a result, poor selectivities and multiple products are often problematic during chemical transformations. One common method employed to improve selectivities in reactions with glycerol is protection via acetalization/ketalization (Scheme 1a), where reaction with an aldehyde/ketone in the presence of a catalyst can generate both five-membered-ring (1,3-dioxolane) or six-membered-ring (1,3-dioxane) products, depending on the hydroxyl groups involved. In addition to behaving as protecting agents, glycerol acetals/ketals have shown promise as fuel additives by increasing the octane number and decreasing gum formation in blended gasolines[5] and reducing the pour point of biodiesel.[6] Acetals/ketals of glycerol also have applications as flavoring agents[7] and surfactants.[8]

Scheme 1

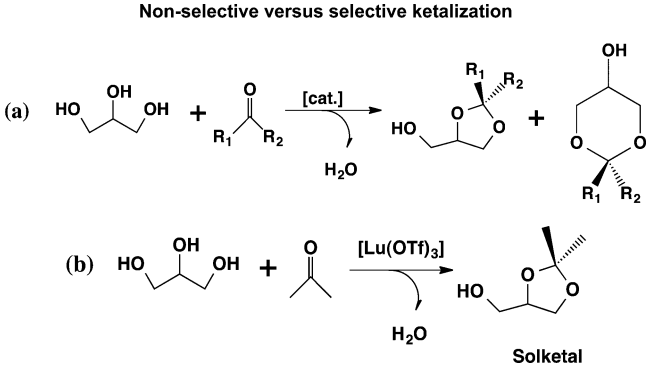

Recent efforts in glycerol acetalization/ketalization have been directed toward the design of catalysts that are regioselective, giving rise to either dioxolane or dioxane formation. A few representative Lewis acid catalysts that are fully selective for formation of the five-membered-ring glycerol ketal with acetone (solketal) are shown in Table 1. Deutsch[9] reported 88% conversion of glycerol over solid Amberlyst-36 in dichloromethane solvent at ∼40 °C (entry 1). In contrast, Mota[10] found Amberlyst-15 to be more efficient (>95% conversion in acetone solution; entry 2) for acetone ketalization, albeit with slightly higher temperatures required (70 °C). Maksimov[11] reported a slightly higher conversion (98%) at 35 °C over zeolite beta in acetone solvent (entry 3). Using a homogeneous Ir catalyst ($[Cp^*IrCl_2]_2$; Cp^* = pentamethylcyclopentadienyl), however,

Received: July 28, 2014
Revised: November 13, 2014
Published: January 12, 2015

 © 2015 American Chemical Society dx.doi.org/10.1021/cs5010932 | ACS Catal. 2015, 5, 1013−1019

Table 1. Lewis Acid Glycerol Ketalization Catalysts Selective for Solketal

catalyst	T (°C)	conversion of glycerol (%)	selectivity for solketal (%)	ref
Amberlyst-36	40	88	100	8
Amberlyst-15	70	>95	100	9
zeolite beta	35	98	100	10
$[Cp^*IrCl_2]_2$	40	86	98	11
$Lu(OTf)_3$	room temp	100	100	17

Crotti[12] found only 86% conversion at 40 °C, with less than full selectivity (98%) for the five-membered ketal (entry 4).

Rare-earth triflates ($Ln(OTf)_3$; $OTf^- = CF_3SO_3^-$) have gained attention as effective Lewis acid catalysts for a wide array of organic reactions.[13] One reason for this is that rare-earth triflates are recyclable. Additionally, these molecules are water-compatible catalysts, an important property for reactions such as acetalization/ketalization, which generate water as a byproduct (Scheme 1). Indeed, $Sc(OTf)_3$,[14] $Ce(OTf)_3$,[15] and $Yb(OTf)_3$[16] are known to catalyze acetalizations/ketalizations under mild conditions. We recently found that $Lu(OTf)_3$ is an efficient catalyst for acetone ketalization with glycerol.[17] Complete conversion of glycerol and acetone into solketal occurred under mild conditions (room temperature) (Table 1, entry 5; Scheme 1b).

Herein, we present DFT calculations for the mechanism of $Lu(OTf)_3$-catalyzed glycerol ketalization with acetone. The "standard" ketalization mechanism (Scheme 2) described in the literature is usually assumed a priori to be sequential; (i) the Lewis acid activates the ketone for polyol binding; (ii) coordination of the polyol to the ketone occurs; (iii) proton transfer occurs to yield a hemiketal; (iv) coordination of another −OH group to the tertiary carbon center occurs; (v) proton transfer to yield the ketal then completes the cycle. Nevertheless, we decided to carry out computational studies for two reasons: first, to our knowledge, computational studies of the mechanism of acetalization/ketalization *with any catalyst* have been absent from the literature, and second, a computational investigation is necessary to understand the kinetic basis for the regioselectivity observed in solketal formation with $Lu(OTf)_3$. In the following section, a model of the $Lu(OTf)_3$ catalyst in solution is rationalized and, after selection of a model catalyst, the ketalization mechanism is presented.

COMPUTATIONAL MODEL

All calculations were carried out with the Gaussian 09 program suite.[18] The DFT functional was chosen by calibration with the CBS-QB3[19] free energies for the total five-membered and six-membered ketalizations (Table 2). Solvent effects (acetone) were included by using the conductor-like polarizable continuum model (CPCM).[20] Natural atomic charges[21] were computed with the NBO 3.1 program as implemented in Gaussian 09. For each reaction (Table 2), the B3LYP[22] values are the worst and improve in the order B3LYP, M06, M06-2X.[23] Since the free energies computed with the latter functional are within 3 kcal/mol of those computed with CBS-QB3 method, the M06-2X functional along with CPCM solvation (acetone) was used for the remainder of this work unless stated otherwise.

The Stuttgart relativistic effective core potential (RECP)[24] was used to replace the innermost 28 electrons of Lu. For the valence electrons of Lu, the contracted Gaussian-type orbital (GTO) basis set (14s13p10d8f6g)/[10s8p5d4f3g] of Dolg[24] was used with modification by removing the tight g functions ((14s13p10d8f)/[10s8p5d4f]). The 6-311+G(d) basis set was used for H, C, and O. All geometries were optimized without symmetry constraints and confirmed as stationary points or transition states by the presence of zero or one imaginary frequency, respectively, in the calculated energy Hessian, and all reported

Scheme 2

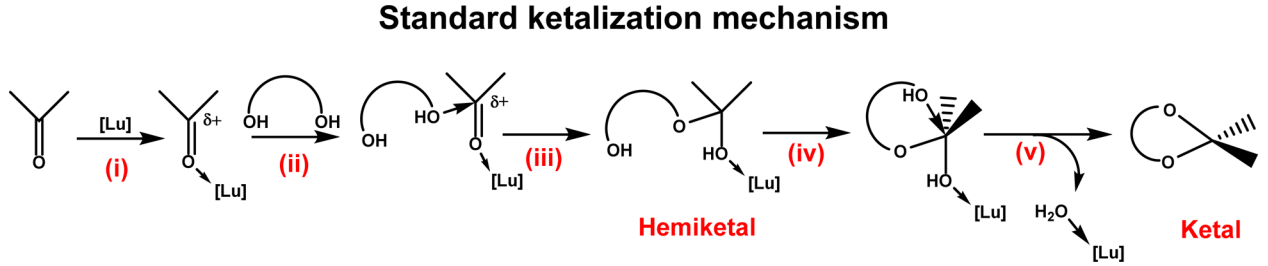

Table 2. Free Energies (kcal/mol) of Acetone Ketalization Computed with Various Methods[a]

	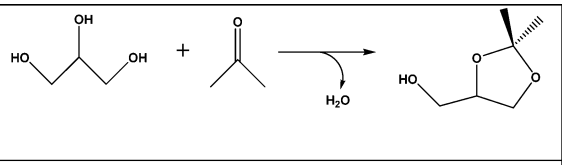	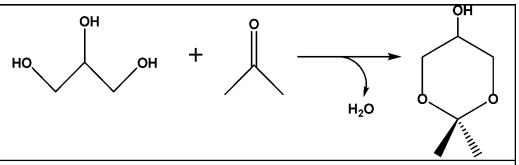
B3LYP	8.23	9.81
M06	3.61	2.88
M06-2X	1.49	-0.18
CBS-QB3	-2.44	-2.54

[a]The 6-311+G(d) basis set was used for each calculation.

dx.doi.org/10.1021/cs5010932 | ACS Catal. 2015, 5, 1013−1019

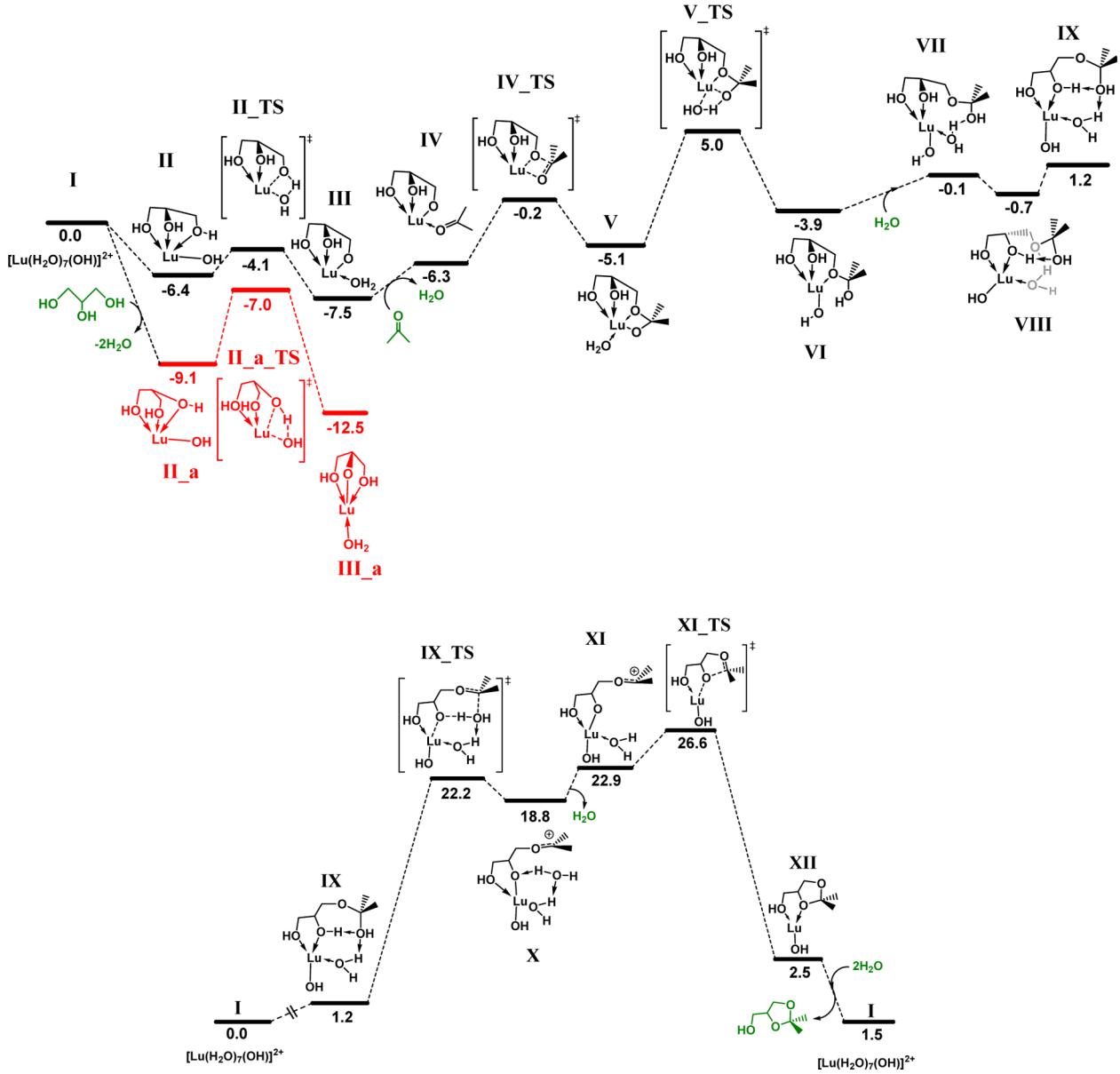

Figure 1. Computed glycerol−acetone ketalization mechanism from glycerol to constrained hemiketal species **IX** (in which the glycerol CH_2OH moiety remains hydrogen bonded to the internal OH group of glycerol, top part of figure) and from the constrained hemiketal **IX** to solketal (bottom part of figure). Free energies (kcal/mol) are computed relative to that of $[Lu(H_2O)_7(OH)]^{2+}$. Each intermediate has an overall charge of +2. The H_2O ligands inactive toward catalysis have been omitted for clarity.

energies correspond to 298.15 K and 1 atm. Intrinsic reaction coordinates (IRCs)[25] were computed for each transition state to verify connectivity with the corresponding reactants and products.

When $Lu(OTf)_3$ is dissolved in aqueous solution, the triflate counterions move into the outer coordination sphere[26] to yield a solution structure that is roughly $[Lu(H_2O)_{8.2}](OTf)_3$, on the basis of X-ray absorption experiments.[27] Although the initial conditions in the acetone ketalization were carried out using 10 mL of acetone, 1 mmol of glycerol, and 1 mol % of $Lu(OTf)_3$ relative to glycerol (i.e., a 136:1:0.01 acetone solvent:glycerol:Lu-$(OTf)_3$ ratio),[17] we initially chose $[Lu(H_2O)_8]^{3+}$ as the model solution species for three reasons (see the Supporting Information for a rationale).

In a study of Lewis acid catalyzed aldol reactions, Kobayashi[28] found that metal cations with pK_h values less than 4 (K_h = hydrolysis constant for $Lu^{3+}(aq) + H_2O \leftrightarrow Lu(OH)^{2+}(aq) + H^+(aq)$ are easily hydrolyzed, whereas those with pK_h values above 10 are not acidic enough to catalyze the aldol reactions. Since Lu^{3+} falls within this range (pK_h = 7.6), it will likely be hydrolyzed to an appreciable extent, especially as the H_2O concentration increases over the course of the ketalization reaction. In fact, the calculated deprotonation free energy of $[Lu(H_2O)_8]^{3+}$ ($[Lu(H_2O)_8]^{3+} \rightarrow [Lu(H_2O)_7(OH)]^{2+} + H^+(aq)$[29]) in water is slightly favorable (−1.49 kcal/mol). Thus, a final modification was made by replacing one H_2O ligand within $[Lu(H_2O)_8]^{3+}$ with OH^- to give $[Lu(H_2O)_7(OH)]^{2+}$ as the model active species used for the remainder of this work.

RESULTS

The computed mechanism for acetone ketalization and metrics for select intermediates are shown in Figures 1 and 2,

dx.doi.org/10.1021/cs5010932 | ACS Catal. 2015, 5, 1013−1019

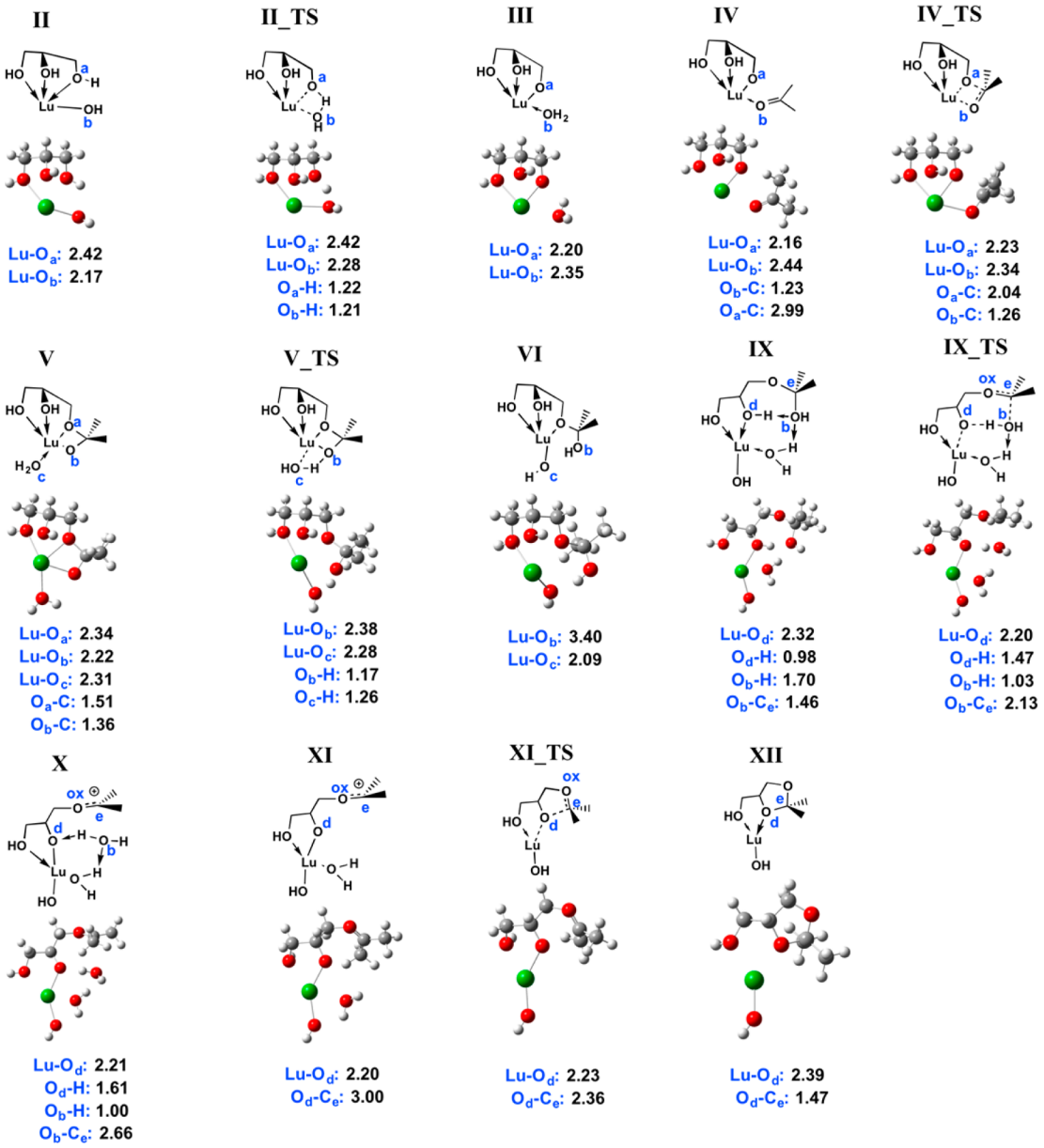

Figure 2. Optimized geometries and metrics for select intermediates in the glycerol acetalization mechanism of Figure 1. The H_2O ligands inactive toward catalysis have been omitted for clarity. Bond lengths are given in Å.

respectively. Coordination of glycerol to $[Lu(H_2O)_7(OH)]^{2+}$ (**I**) in a κ^3*O,O,O* mode to displace two H_2O molecules such that the terminal (**II**) or internal (**II_a**) hydroxyl is adjacent to the Lu−OH ligand is exergonic (ΔG = −6.4 and −9.1 kcal/mol, respectively), giving $[Lu(H_2O)_5(OH)(\kappa^3\text{-glycerol})]^{2+}$. Proton transfer from the glycerol −OH to the Lu−OH group is again exergonic (ΔG = −1.1 (**III**) and −3.4 kcal/mol (**III_a**)), leading to the terminally (**III**) or internally (**III_a**) deprotonated glycerol complex $[Lu(H_2O)_6(O\text{-glycerol})]^{2+}$. The barriers for hydrogen transfer are small ($\Delta G^{\ddagger}$ = 2.3 (**II_TS**) and 2.1 kcal/mol (**II_a_TS**)).

Although internal deprotonation of glycerol (**III_a**) from $[Lu(H_2O)_7(OH)]^{2+}$ is thermodynamically and kinetically preferred to terminal deprotonation (**III**), the computed mechanism is continued for only the latter pathway for two reasons: First, primary hydroxyl group deprotonation (**I** → **III**) is also energetically feasible, and second, after hemiketal formation via the internally deprotonated oxygen of the glycerol intermediate **III_a**, ketalization can only occur with either of the two terminal hydroxyl groups to give exclusively the five-membered-ring solketal (Scheme 3). *Thus, only terminal (primary −OH group) glycerol deprotonation is considered in order to account for the possibility of six-membered-ring (1,3-dioxane) formation in addition to the solketal.*

Displacement of the newly formed Lu−(OH_2) ligand of **III** with acetone (ΔG = 1.2 kcal/mol) to give **IV** ($[Lu(H_2O)_5(\text{acetone})(O\text{-glycerol})]^{2+}$) is slightly endergonic (ΔG = 1.2 kcal/mol), consistent with the poorer basicity of acetone. The acetone ligand can bend toward the deprotonated glycerol O ligand and undergo C−O coupling ($\Delta G^{\ddagger}$ = 6.1 kcal/mol) to yield the coupled intermediate **V** ($[Lu(H_2O)_5(O\text{-acetone-glycerol})]^{2+}$), which is again slightly endergonic (ΔG = 1.2 kcal/mol) relative to **IV**. During C−O coupling, the O_a−Lu−O_b angle decreases from 74.25° (**IV**) to 66.00° (**IV_TS**) and finally to 58.24° (**V**) with a concomitant decrease in the Lu−O_b (2.44 Å (**IV**), 2.34 Å (**IV_TS**), 2.22 Å (**V**)) and C−O_a (2.99 Å (**IV**), 2.04 Å (**IV_TS**),

dx.doi.org/10.1021/cs5010932 | *ACS Catal.* 2015, 5, 1013−1019

Scheme 3

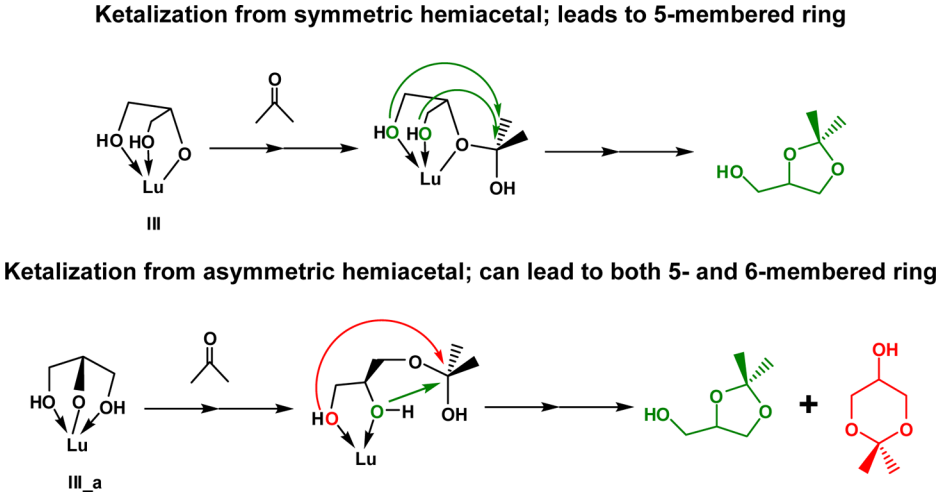

1.51 Å (**V**)) bond distances (Figure 2). A second proton transfer from another Lu-bound water ligand to the acetone O atom to yield the hemiketal **VI** ($[Lu(H_2O)_4(OH)(hemiketal)]^{2+}$) is endergonic ($\Delta G$ = 1.2 kcal/mol), with a free energy barrier of 10.1 kcal/mol (**V_TS**). The higher barrier and total free energy for this deprotonation are more positive than those for glycerol OH deprotonation ($\Delta G^{\ddagger}$(**II** → **II_TS**) = 2.3 kcal/mol; ΔG(**II** → **III**) = −1.1 kcal/mol). This discrepancy arises from the fact that the Lu-bound OH ligand of **II** remains coordinated to Lu following proton transfer from glycerol (Lu−O_b: 2.17 Å (**II**), 2.28 Å (**II_TS**), 2.35 Å (**III**); Figure 2), whereas no Lu−O_b coordination is present in **VI** following proton transfer from a Lu-bound water ligand (Lu−O_b: 2.22 Å (**V**), 2.38 Å (**V_TS**), 3.40 Å (**VI**); Figure 2).

In the classical ketalization mechanism (Scheme 2), ketal formation from the hemiketal involves deprotonation of a second glycerol hydroxyl group and protonation/dehydration of the 2-propanol group. These two steps can occur in a concerted fashion following conformational isomerism of hemiketal **VI**. Displacing the hydroxyl-substituted ether linkage from the coordination sphere of Lu with an added water molecule to yield **VII** ($Lu(H_2O)_5(OH)(hemiketal)]^{2+}$), in which the hemiketal −OH ligand coordinates to a Lu-bound H_2O molecule, is endergonic (ΔG = 3.8 kcal/mol). Coordination of the hemiketal −OH group to the hydrogen atom of the secondary −OH of the bound glycerol moiety (ΔG(**VII** → **VIII**) = −0.6 kcal/mol) followed by coordination to a Lu-bound H_2O molecule (ΔG(**VIII** → **IX**): = 1.9 kcal/mol) to yield the constrained hemiketal **IX** is approximately thermoneutral.[30] From hemiketal **IX**, proton transfer from the secondary −OH group to the propanol −OH fragment and propanol dehydration occur in the same step to provide the oxonium intermediate **X** (ΔG(**IX** → **X**) = 17.6 kcal/mol). This species contains the H_2O molecule generated by propanol dehydration coordinated to both the secondary glycerol oxygen atom and a Lu−(OH_2) ligand (i.e. $[Lu(H_2O)_5(OH)(H_2O)(oxonium)]^{2+}$). In the transition state **IX_TS** to the oxonium species **X**, proton transfer is nearly complete, with the O_d−H (0.98 Å (**IX**), 1.47 Å (**IX_TS**), 1.61 Å (**X**)) and O_b−H (1.70 Å (**IX**), 1.03 Å (**IX_TS**), 1.00 Å (**X**)) distances differing from those of **X** by 0.14 and 0.03 Å, respectively (Figure 2). Although the degree of propanol dehydration in **IX_TS** is not as advanced as that for H atom transfer, the O_b−C_e distance (1.46 Å (**IX**), 2.13 Å (**IX_TS**), 2.66 Å (**X**); Figure 2) is still closer to that of the oxonium species. Due to the lateness of the transition state, the barrier to the oxonium intermediate (21.0 kcal/mol) is significantly higher than those for the previous steps. Both the higher barriers and total free energies required to form oxonium ion intermediates also correlate with the increase in positive charge on forming the oxonium group (C_e, O_{ox}). This is confirmed by the computed natural atomic charges, which become more positive for **IX_TS** (Δq = +0.075 (C_e), +0.056 (O_{ox})) and **X** (Δq = +0.087 (C_e), +0.083 (O_{ox})) relative to the constrained hemiketal **IX**.

In order to form the solketal, the coordinated H_2O formed from the transformation of **IX** into **X** must be removed (ΔG(**X** → **XI**) = 4.1 kcal/mol) to give the oxonium species **XI** ($[Lu(H_2O)_5(OH)(oxonium)]^{2+}$), followed by C−O coupling between the acetone carbon atom and the secondary glycerol oxygen atom. The formation of the $\kappa^2 OH,O$ solketal adduct **XII** is exothermic (ΔG(**XI** → **XII**) = −20.4 kcal/mol), with a small barrier for ring closure ($\Delta G^{\ddagger}$ = 3.7 kcal/mol). That the free energy change for ring closure (**XI** → **XII**) has a similar magnitude but opposite sign in comparison to that of propanol dehydration (**IX** → **X**) is consistent with the change in natural atomic charges on the oxocarbenium moiety (C_e,O_{ox}), as the oxocarbenium group is broken (Δq(**XI** → **XII**) = −0.063 (C_e), −0.084 (O_{ox})) and formed (Δq(**IX** → **X**) = +0.087 (C_e), +0.083 (O_{ox})), respectively. Furthermore, the ring closure proceeds through an early transition state, as the O_d−C_e (3.00 Å (**XI**), 2.36 Å (**XI_TS**), 1.47 Å (**XII**); Figure 2) and Lu−O_d (2.20 Å (**XI**), 2.23 Å (**XI_TS**), 2.39 Å (**XII**); Figure 2) distances in **XI_TS** are closer to those of the reactant **XI**. Finally, release of solketal via displacement with two H_2O molecules to close the catalytic cycle and regenerate the initial active hydroxyl species **I** is exergonic by 1.0 kcal/mol.

DISCUSSION

When the secondary glycerol −OH group is deprotonated, the experimentally observed selectivity for the five-membered-ring solketal during glycerol ketalization is inevitable in light of the symmetry of intermediate **III** (Scheme 3). On the other hand, when a primary glycerol −OH group is initially deprotonated, the selectivity for solketal is explicable in terms of the constrained hemiketal **IX** in the computed mechanism (Figure 1), wherein the propanol group is poised to abstract the hydrogen atom from the secondary −OH group of glycerol. Formation of the

dx.doi.org/10.1021/cs5010932 | ACS Catal. 2015, 5, 1013−1019

Scheme 4

Proposed pathway for formation of dioxane

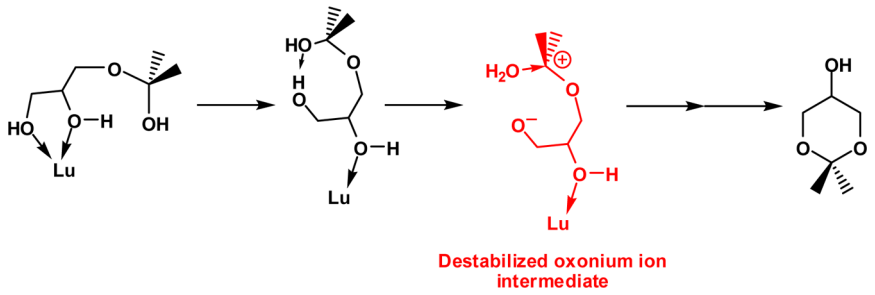

Destabilized oxonium ion intermediate

six-membered-ring dioxane, on the other hand, would require hydrogen transfer from the primary −OH group of glycerol to the propanol group. However, manipulation of the propanol group to form the analogous constrained hemiketal, in which propanol forms a hydrogen-bonding interaction with the primary glycerol −OH group, proved to be impossible without twisting the latter group and breaking the Lu←OH dative bond (Scheme 4). As the corresponding oxonium intermediate forms via hydrogen transfer/deprotonation, negative charge accumulates on the primary glycerol oxygen atom, which is no longer bound to the Lu center. Thus, the corresponding transition state and oxonium ion intermediate should be significantly destabilized, and six-membered-ring dioxane formation can be ruled out on that basis.

The rate-limiting step of the glycerol ketalization is either oxocarbenium formation or acetal formation ($\Delta G^{\ddagger}$(**I** → **IX_TS**) = 22.2 kcal/mol; $\Delta G^{\ddagger}$(**I** → **XI_TS**) = 26.6 kcal/mol, respectively) on the basis of the similar barriers computed for both steps. Additionally, the free energies of the two oxocarbenium intermediates relative to $[Lu(H_2O)_7(OH)]^{2+}$ are similar in magnitude (ΔG(**I** → **X**) = 18.8 kcal/mol; ΔG(**I** →**XI**) = 22.9 kcal/mol). While the computed free energies are high for a ketalization reaction that is complete after approximately 60−180 min at room temperature (Table 1, entry 5),[17,17b] our computations neglect the effects of explicit solvent molecules in stabilizing the oxonium ion, which may lower these values. Furthermore, absolute free energies are computed in Gaussian09 for standard conditions (1 M of each species in solution). If these values are corrected for the use of excess acetone as a reactant, we predict the barrier to be much lower.[31] Although the assumption that ketal formation in aqueous solution proceeds from a hemiketal via an oxonium intermediate is not always valid,[32] we believe the oxonium cation $ROC(CH_3)_2^+$ in **X** and **XI** will have a sufficient lifetime to serve as an intermediate on the basis of the fact that the smaller oxocarbenium analogue $MeOC(CH_3)_2^+$ has a hydrolysis constant (k_{HOH}) of 1×10^9 s^{-1} [33] and thus has a lifetime 4 orders of magnitude longer than a bond vibration ($\sim 10^{-13}$ s).

In contrast to the classical ketalization mechanism (Scheme 2), glycerol −OH deprotonation (**II** → **III**) occurs prior to glycerol−acetone C−O coupling (**IV** → **V**) in the computed mechanism. The reordering of both steps was found necessary to facilitate C−O coupling, as the adduct in which the glycerol −OH moiety coordinates to the acetone C═O carbon (Scheme 2, step iii) was found to be unstable during geometry optimization. Additionally, glycerol −OH group deprotonation should occur readily, as the barriers are quite low (2.1−2.3 kcal/mol; Figure 1). The conversion of hemiketal **IX** into ketal **XII** also takes place via a mechanism different from that shown in Scheme 2. Instead of a contortion of either glycerol $-CH_2OH$ group away from Lu to displace the propanol −OH fragment in an S_N2 fashion (Scheme 2, step v), direct proton transfer and propanol dehydration occur in a concerted fashion (**IX** → **X**).[34]

A possible competitive process involves the Lu−OH + H^+ ↔ $Lu-OH_2$ equilibrium, which was invoked to justify the use of $[Lu(H_2O)_7(OH)]^{2+}$ as the active species for glycerol ketalization. However, this equilibrium is only relevant for the κ^3O,O,O glycerol complexes **II** and **II_a**, since the Lu−OH group is only needed to facilitate the initial glycerol −OH group deprotonation. From hemiketal **VI** onward, the Lu−OH ligand is not directly involved in the catalysis, and thus the equilibrium should not substantially affect the intermediates in the later portion of the mechanism.

Finally, despite the computational evidence presented for the mechanism of Lu triflate catalyzed glycerol ketalization with acetone shown in Figure 1, we cannot unequivocally confirm it without more detailed kinetic studies and computations to shed additional light on the nature of the active species under the reaction conditions (*assumed to be* $[Lu(H_2O)_7(OH)]^{2+}$ *in this work*), additional reaction intermediates accessible at room temperature, and the role of explicit solvent molecules in stabilizing intermediates such as the various oxonium species formed.

CONCLUSIONS

A mechanism for the $Lu(OTf)_3$-catalyzed glycerol ketalization with acetone was computed in order to address the observed experimental regioselectivity for the five-membered-ring product (solketal). When ketalization occurs via the secondary −OH group of glycerol, *only solketal formation should be possible due to the symmetry of the intermediates*. Ketalization via the terminal (primary) −OH group of glycerol is predicted to occur in a different manner than the conventional ketalization mechanism. After coordination of glycerol to Lu (**I** → **II**), a terminal (primary) glycerol −OH moiety is deprotonated (**II** → **III**) and a Lu-bound water ligand is displaced with acetone (**III** → **IV**). After C−O coupling between acetone and glycerol (**IV** → **V**), proton transfer occurs between a Lu-bound water ligand and the acetone oxygen center to give a hemiketal (**V** → **VI**). Ligand rearrangement through several intermediates yields a constrained hemiketal (**VI** → **IX**), which is invoked to explain the stereoselectivity for solketal formation. Finally, after the reaction proceeds through a rate-limiting step involving oxonium ion intermediates, solketal is formed (**IX** → **XII**) and displaced by water (**XII** → **I**) to complete the catalytic cycle.

dx.doi.org/10.1021/cs5010932 | *ACS Catal.* 2015, 5, 1013−1019

■ ASSOCIATED CONTENT

Supporting Information

The following file is available free of charge on the ACS Publications website at DOI: 10.1021/cs5010932.

Model systems chosen for computations as well as *xyz* coordinates (PDF)

■ AUTHOR INFORMATION

Corresponding Author

*E-mail for A.W.P.: awp319.aol.com.
*E-mail for J.C.G.: jgordon@lanl.gov.

Present Addresses

[‖](For W.C.) Philips (China) Investment Co. Ltd., Shanghai 200233, People's Republic of China.
[⊥](For J.K.K.) Samyang Genex Corp., Daejeon 305 717, South Korea.
[#](For C.B.H.) School of Chemical & Biomolecular Engineering, Georgia Institute of Technology, Atlanta, GA 30332, USA.

Notes

The authors declare no competing financial interest.

■ ACKNOWLEDGMENTS

We to thank the LANL Laboratory Directed Research and Development Program for financial support.

■ REFERENCES

(1) Gupta, R. B.; Demirbas, A. *Gasoline, Diesel, and Ethanol Biofuels from Grasses and Plants*; Cambridge: New York, 2010; pp 109−110.

(2) U.S. Energy Information Administration/International Energy Statistics. http://www.eia.gov/cfapps/ipdbproject/IEDIndex3.cfm?tid=79=79=1 (accessed June 2014).

(3) (a) Willke, T.; Vorlop, K.-D. *Appl. Microbiol. Biotechnol.* **2004**, *66*, 131−142. (b) Dharmadi, Y.; Murarka, A.; Gonzalez, R. *Biotechnol. Bioeng.* **2006**, *94*, 821−829.

(4) (a) Zhou, C.; Beltramini, J. N.; Fan, Y.; Lu, G. Q. *Chem. Soc. Rev.* **2008**, *37*, 527−549. (b) Chai, S. H.; Wang, H. P.; Liang, Y.; Xu, B. Q. *J. Catal.* **2007**, *250*, 342−349. (c) Dasari, M. A.; Kiatsimkul, P. P.; Sutterlin, W. R.; Suppes, G. J. *Appl. Catal., A: Gen.* **2005**, *281*, 225−231. (d) Gray, P.; Williams, A. *Nature* **1960**, *188*, 56−56. (e) Klepáčová, K.; Mravec, D.; Bajus, M. *Appl. Catal., A: Gen.* **2005**, *294*, 141−147. (f) Soares, R. R.; Simonetti, D. A.; Dumesic, J. A. *Angew. Chem., Int. Ed.* **2006**, *45*, 3982−3985.

(5) Mota, C. J. A.; da Silva, C. X. A.; Rosenbach, N.; Costa, J.; da Silva, F. *Energy Fuels* **2010**, *24*, 2733−2736.

(6) (a) De Torres, M.; Jiménez-osés, G.; Mayoral, J. A.; Pires, E.; de los Santos, M. *Fuel* **2012**, *94*, 614−616. (b) Silva, P. H. R.; Gonçalves, V. L. C.; Mota, C. J. A. *Biores. Technol.* **2010**, *101*, 6225−6229.

(7) (a) Climent, M. J.; Corma, A.; Velty, A. *Appl. Catal., A: Gen.* **2004**, *263*, 155−161. (b) Climent, M. J.; Velty, A.; Corma, A. *Green Chem.* **2002**, *4*, 565−569.

(8) Sokołowski, A.; Piasecki, A.; Burczyk, B. *J. Am. Oil Chem. Soc.* **1992**, *69*, 633−638.

(9) Deutsch, J.; Martin, A.; Lieske, H. *J. Catal.* **2007**, *245*, 428−435.

(10) da Silva, C. X. A.; Gonçalves, V. L. C.; Mota, C. J. A. *Green Chem.* **2009**, *11*, 38−41.

(11) Maksimov, A. L.; Nekhaev, A. I.; Ramazanov, D. N.; Arinicheva, Y. A.; Dzyubenko, A. A.; Khadzhiev, S. N. *Pet. Chem.* **2011**, *51*, 61−69.

(12) Crotti, C.; Farnetti, E.; Guidolin, N. *Green Chem.* **2010**, *12*, 2225−2231.

(13) (a) Kobayashi, S.; Sugiura, M.; Kitagawa, H.; Lam, W. W.-L. *Chem. Rev.* **2002**, *102*, 2227−2302. (b) Ladziata, U. *ARKIVOK* **2014**, 307−336.

(14) Pozsgay, V. *Tetrahedron: Asymmetry* **2000**, *11*, 151−172.

(15) (a) Ono, F.; Takenaka, H.; Fujikawa, T.; Mori, M.; Sato, T. *Synthesis* **2009**, *8*, 1318−1322. (b) Ono, F.; Inatomi, Y.; Tada, Y.; Mori, M.; Sato, T. *Chem. Lett.* **2009**, *38*, 96−97.

(16) Li, G.-Q.; Shan, W.-G.; Su, W.-K.; Yao, Z.-J. *Chin. J. Chem.* **2007**, *25*, 90−94.

(17) Kim, J. K.; Chen, W.; Hoyt, C. B.; Michalczyk, R.; Scott, B. L.; Silks III, L. A; Sutton, A. D. Wu, R.; Gordon, J. C. Unpublished results. (b) The rate of conversion of acetone and glycerol into the solketal at room temperature in the presence of $Lu(OTf)_3$ appears to be variable depending on the source of glycerol and acetone (e.g. ∼1−3 h). We believe that this may be due to varying degrees of water present in solution. Regardless, we have not observed the formation of any six-membered (1,3-dioxane) product in the course of our studies..

(18) Frisch, M. J.; Trucks, G. W.; Schlegel, H. B.; Scuseria, G. E.; Robb, M. A.; Cheeseman, J. R.; Scalmani, G.;Barone, V.; Mennucci, B.; Petersson, G. A.; Nakatsuji, H.; Caricato, M.; Li, X.; Hratchian, H. P.; Izmaylov, A. F.; Bloino, J.; Zheng, G.; Sonnenberg, J. L.; Hada, M.; Ehara, M.; Toyota, K.; Fukuda, R.; Hasegawa, J.; Ishida, M.; Nakajima, T.; Honda, Y.; Kitao, O.; Nakai, H.; Vreven, T.; Montgomery, J. A., Jr.; Peralta, J. E.; Ogliaro, F.; Bearpark, M.; Heyd, J. J.; Brothers, E.; Kudin, K. N.; Staroverov, V. N.; Kobayashi, R.; Normand, J.; Raghavachari, K.; Rendell, A.; Burant, J. C.; Iyengar, S. S.; Tomasi, J.; Cossi, M.; Rega, N.; Millam, N. J.; Klene, M.; Knox, J. E.; Cross, J. B.; Bakken, V.; Adamo, C.; Jaramillo, J.; Gomperts, R.; Stratmann, R. E.; Yazyev, O.; Austin, A. J.; Cammi, R.; Pomelli, C.; Ochterski, J. W.; Martin, R. L.; Morokuma, K.; Zakrzewski, V. G.; Voth, G. A.; Salvador, P.; Dannenberg, J. J.; Dapprich, S.; Daniels, A. D.; Farkas, Ö.; Foresman, J. B.; Ortiz, J. V.; Cioslowski, J.; Fox, D. J. *Gaussian 09, Revision B.01*; Gaussian, Inc., Wallingford, CT, 2009.

(19) (a) Montgomery, J. A., Jr.; Frisch, M. J.; Ochterski, J. W.; Petersson, G. A. *J. Chem. Phys.* **1999**, *110*, 2822−2827. (b) Montgomery, J. A., Jr.; Frisch, M. J.; Ochterski, J. W.; Petersson, G. A. *J. Chem. Phys.* **2000**, *112*, 6532−6542.

(20) (a) Barone, V.; Cossi, M. *J. Phys. Chem. A* **1998**, *102*, 1995−2001. (b) Cossi, M.; Rega, N.; Scalmani, G.; Barone, V. *J. Comput. Chem.* **2003**, *24*, 669−681.

(21) (a) Reed, A. E.; Weinhold, F. *J. Chem. Phys.* **1983**, *78*, 4066−4073. (b) Reed, A. E.; Weinstock, R. B.; Weinhold, F. *J. Chem. Phys.* **1985**, *83*, 735−746.

(22) (a) Becke, A. D. *J. Chem. Phys.* **1993**, *98*, 1372−1378. (b) Becke, A. D. *J. Chem. Phys.* **1993**, *98*, 5648−5652.

(23) Zhao, Y.; Truhlar, D. G. *Theor. Chem. Acc.* **2008**, *120*, 215−241.

(24) Cao, X.; Dolg, M. *J. Mol. Struct. (THEOCHEM)* **2002**, *581*, 139−147.

(25) Fukui, K. *Acc. Chem. Res.* **1981**, *14*, 363−368.

(26) Abbasi, A.; Lindqvist-Reis, P.; Eriksson, L.; Sandström, D.; Lidin, S.; Persson, I.; Sandström, M. *Chem.—Eur. J.* **2005**, *11*, 4065−4077.

(27) D'Angelo, P.; Zitolo, A.; Migliorati, V.; Persson, I. *Chem. Eur. J.* **2010**, *16*, 684−692.

(28) Kobayashi, S.; Manabe, K. *Acc. Chem. Res.* **2002**, *35*, 209−217 and references therein .

(29) An empirical value for the proton solvation free energy was used. See: Liptak, M. D.; Gross, K. C.; Seybold, P. G.; Feldgus, S.; Shields, G. C. *J. Am. Chem. Soc.* **2002**, *124*, 6421−6427.

(30) Transition states were not found among intermediates **VI**−**IX**.

(31) If this is not the case, solketal should form via internal glycerol OH deprotonation (Figure 2, **II_a** → **III_a** etc.)

(32) (a) Young, P. R.; Jencks, W. P. *J. Am. Chem. Soc.* **1977**, *99*, 8238−8248. (b) Kniew, B. L.; Jencks, W. P. *J. Am. Chem. Soc.* **1980**, *102*, 6789−6798.

(33) Amyes, T. L.; Jencks, W. P. *J. Am. Chem. Soc.* **1989**, *111*, 7888−7900.

(34) Formation of an oxocarbenium intermediate is not inconsistent with the classical mechanism and may occur as a substep of step v in Scheme 2.